Inorganic Chemistry

pubs.acs.org/IC

Article

Sound Velocities, Elasticity, and Mechanical Properties of Stoichiometric Submicron Polycrystalline δ-MoN at High Pressure

Yongtao Zou,* Ke Liu, Pei Wang, Daowei Wang, Mu Li, Ying Li, Leiming Fang,* Hongbin Zhuo, Shuangchen Ruan,* Cangtao Zhou,* and Yusheng Zhao

Cite This: https://doi.org/10.1021/acs.inorgchem.1c00406

Read Online

ACCESS | Metrics & More | Article Recommendations | Supporting Information

ABSTRACT: Acoustic velocities and elasticity of stoichiometric submicron polycrystalline δ-MoN have been reported at high pressure using ultrasonic measurements and first-principles calculations. Using the finite-strain equation-of-state approach, the bulk modulus and shear rigidity, as well as their pressure derivatives, are derived from the current experimental data, yielding B_{S0} = 360.0(8) GPa, G_0 = 190.0(5) GPa, $\partial B_S/\partial P$ = 3.4(2), and $\partial G/\partial P$ = 1.4(1). Based on our experimental data and the velocity−elasticity correlated models, the mechanical/thermal properties (*i.e.*, hardness, fracture toughness, Grüneisen parameter, Debye temperature, Poisson's ratio) are also derived. Interestingly, we find that hexagonal δ-MoN is almost as incompressible as superhard cubic boron nitride (cBN) (∼384 GPa) and its hexagonal ε-NbN (∼373 GPa) counterpart, and its shear rigidity (G = 190 GPa) is comparable to that of the superhard diamond composite (G = 204 GPa). Moreover, the fracture toughness of submicron δ-MoN polycrystals is achieved up to ∼4.3 MPa·m$^{1/2}$, which is comparable to superhard diamond (4−7 MPa·m$^{1/2}$) and cBN (2−5 MPa·m$^{1/2}$). The Vickers hardness of submicron δ-MoN is estimated to be $H_v \approx$ 17.4 GPa using Chen's model, which is found to be almost as hard as hexagonal ε-NbN and δ-WN, and may be very important for its applications in extreme environments.

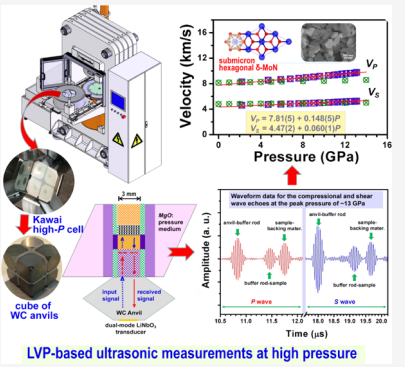

INTRODUCTION

Transition-metal nitrides have attracted great interest in inorganic chemistry, condensed matter physics, and materials science due to their superior properties such as incompressibility, high hardness, high melting point, good thermal stability, and superconductivity with relatively high-critical temperatures (T_c).[1−14] It is known that most of the early transition-metal nitrides favor its crystallization into rocksalt structured mononitrides, while some of their heavy-metal counterparts prefer to adopt zinc-blend or hexagonal structures, such as δ-MoN and ε-NbN.[4,5,15] Among these nitrides, δ-MoN adopts an unusual hexagonal structure ($P6_3mc$: no. 186) under ambient conditions with a three-dimensional cation−anion network, and possesses high hardness and relatively high-critical temperatures (T_c).[15−19]

It is well accepted that elastic moduli and their pressure derivatives of materials are important parameters to unravel the correlations between structural evolution and physical properties.[20,21] Previous first-principles calculations revealed that hexagonal δ-MoN is energetically more stable than its rocksalt-structured γ-MoN counterpart.[17,18] Previous static compression experiments and theoretical calculations showed that the bulk modulus of δ-MoN is ranging from 345 to 379 GPa,[15,17,22,23] which is almost the same value as that of cubic γ-MoN (∼351 GPa) by Kanoun et al.,[23] and also comparable to $B_0 \approx$ 384 GPa for superhard cubic boron nitride (cBN).[24] Recently, Wang et al.[19] performed hardness measurements on hexagonal δ-MoN using a Vickers indenter, indicating a pronounced load dependence of the Vickers hardness. The value of Vickers hardness of δ-MoN was determined to be ∼30 GPa at a relatively low load of ∼0.5 N without giving the asymptote of hardness. This value was ∼30% higher than the reported value of ∼23 GPa for cubic NaCl-type γ-MoN under the same loading.[19] We thus proposed that much higher loads are needed for the growth of microcracks in a brittle material, yielding a reliable hardness value for the bulk δ-MoN, as ever suggested by Zhao et al.[25] and Brazhkin et al.[26]

We know that bulk and shear moduli may be a good predictor to obtain elasticity-correlated mechanical and thermal properties such as Young's modulus, fracture toughness, Vickers hardness, Debye temperature, and Grüneisen parameter if the plastic deformation of materials is considered.[27−30] For example, the ratio of bulk modulus to shear rigidity (B/G) can be applied to evaluate the ductility or brittleness of materials.[31] Despite the importance, almost all previous experimental studies on the elasticity of δ-MoN are

Received: February 8, 2021

focused on the equation of state (EOS) or bulk modulus/compressibility by static compression experiments combined with synchrotron X-ray diffraction observations, only providing the structural stability and compressibility under high pressure, without information about the shear-related properties.[15,17,19,22,23]

Recently, our newly developed technique of in-house ultrasonic measurements in a large volume press (LVP) enabled precise measurements of compressional and shear wave velocities, elasticity at high pressure when synchrotron X-ray/neutron beams are not available.[5,20,21,32,33] In this work, for the first time, we report sound velocities, elasticity, and elasticity-related properties of stoichiometric δ-MoN polycrystals under high pressure using LVP-based ultrasonic measurement techniques complemented with first-principles calculations. The compressional (V_P) and shear (V_S) wave velocities of δ-MoN are measured at pressures up to ~13 GPa, from which the bulk and shear moduli, their pressure derivatives, and elasticity-correlated mechanical/thermal properties are derived, as compared with the results from our theoretically predicted results and previous studies.

EXPERIMENTAL AND THEORETICAL DETAILS

High *P*–*T* Synthesis and Characterization. The stoichiometric hexagonal δ-MoN powders are fabricated at 5–5.5 GPa and 1300 °C with a duration of 5–10 min in a hinge-type large volume press[19] through a high-pressure solid-state metathesis reaction of a mixture of Na_2MoO_4 (~99.5%) and hexagonal boron nitride (hBN) (>99.9%) powders with a molar ratio of 1:2, which is described in eq 1

$$Na_2MoO_4 + 2BN = MoN + 2NaBO_2 + 1/2N_2 \quad (1)$$

The prepared run products were purified using pure water to remove excess Na_2MoO_4 and $NaBO_2$ by-products, and then placed in a high-temperature oven for drying at ~350 K. To obtain high-quality specimens for high-pressure ultrasonic measurements, the stoichiometric polycrystalline bulk δ-MoN were synthesized at ~10 GPa and 1100 °C for 30 min in a Walker-type high-pressure press using the as-prepared δ-MoN powders as the starting material. The well-sintered polycrystalline δ-MoN bulk specimens were characterized by energy-dispersive X-ray diffraction (XRD) at the X17B2 beamline at NSLS, scanning electron microscopy-energy-dispersive X-ray (SEM-EDX: NovaNano at SUStech), and Archimedes density measurements.

High-Pressure Ultrasonic Measurements. Sound velocities of compressional and shear waves for polycrystalline δ-MoN at high pressure have been simultaneously measured in a multi-anvil large volume press. A schematic high-pressure cell assembly used for the current ultrasonic measurements is shown in Figure 1a. Briefly, a piece of $LiNbO_3$ foil with 10° Y cut was used as a transducer, which was mounted on a well-polished truncated face of a tungsten carbide (WC) cubic anvil for receiving and generating compressional and shear wave echoes at various pressures.

To reduce the acoustic energy loss, all surfaces of the transducer-mounted WC anvil, Al_2O_3 buffer rod, and δ-MoN specimen were well-polished using diamond paste with a grain size of 1 μm. Travel times for the compressional (P) and shear (S) waves were simultaneously measured with standard errors of 0.2 and 0.4 ns, respectively.[20,21,32,33] In this study, polycrystalline alumina acted as both a pressure marker and a buffer rod, which was embedded between the δ-MoN specimen and the WC cubic anvil. Based on the travel times of shear waves *vs* pressures for the Al_2O_3 buffer rod, the current cell pressures were calibrated.[33] To obtain a (quasi)-hydrostatic environment for the δ-MoN sample, a very soft cell assembly (soft Sn rod as the backing material) was designed and used in this in-house ultrasonic measurement experiment, instead of heating/annealing the conventional "high-temperature cell assembly" to relax/reduce internal stress/strain when synchrotron X-ray/neutron beams are available.[5,33]

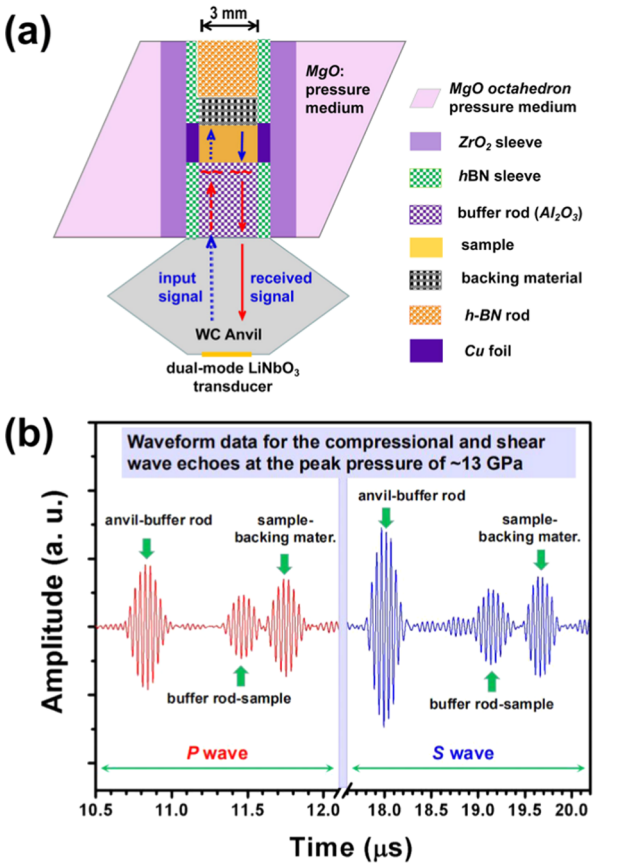

Figure 1. (a) Experimental cell assembly for the current in-house sound velocity measurements at high pressure in a multi-anvil apparatus. (b) Waveform data of the compressional (50 MHz) and shear (30 MHz) wave echoes for submicron polycrystalline δ-MoN at a peak pressure of ~13 GPa, exhibiting the echoes from the interfaces of the WC cubic anvil, the Al_2O_3 buffer rod and the δ-MoN specimen, respectively.

Based on the pre-measured initial sample length and the zero-pressure density, the corresponding sample lengths under various pressures can be estimated by Cook's equation, which is described as a function of the travel times for both the compressional and shear waves.[5,33] After measuring the sample length of the recovered sample, we find that the change in the sample length is within ±1 μm as compared to the initial value, indicating that almost no plastic deformation occurred during the current experiments. Elasticity of bulk modulus and shear rigidity and their pressure dependences are fitted by applying the third-order finite-strain equations. Uncertainties in the bulk and shear moduli are within ~1.5%.[5,20,21,32,33] Representative acoustic signals of the compressional and shear waves for polycrystalline δ-MoN at the maximum pressure of ~13 GPa are shown in Figure 1b. Echoes from the different interfaces (*i.e.*, the WC anvil-buffer rod interface, the buffer rod-sample interface, and the sample-backing material interface) can be clearly observed and identified, which ensures precise measurement of the travel times even at the highest pressure.

First-Principles Calculations. In the current theoretical calculations, interactions between ionic cores and electrons are determined by applying ultrasoft pseudo-potentials. Exchange-correlation potentials are performed by the generalized gradient approximation (GGA) of density functional theory (DFT).[34,35] For the pseudo-potential calculation, the valence electron densities are defined as Mo ($4d^5 5s^1$) and N ($2s^2 2p^3$). The electronic wave functions are treated as a plane wave basis with a cut-off energy of 500 eV. The corresponding Monkhorst–Pack k-points are set to be 10 × 10 × 9. At a certain external pressure/stress, full optimization of the cell should be

https://doi.org/10.1021/acs.inorgchem.1c00406
Inorg. Chem. XXXX, XXX, XXX–XXX

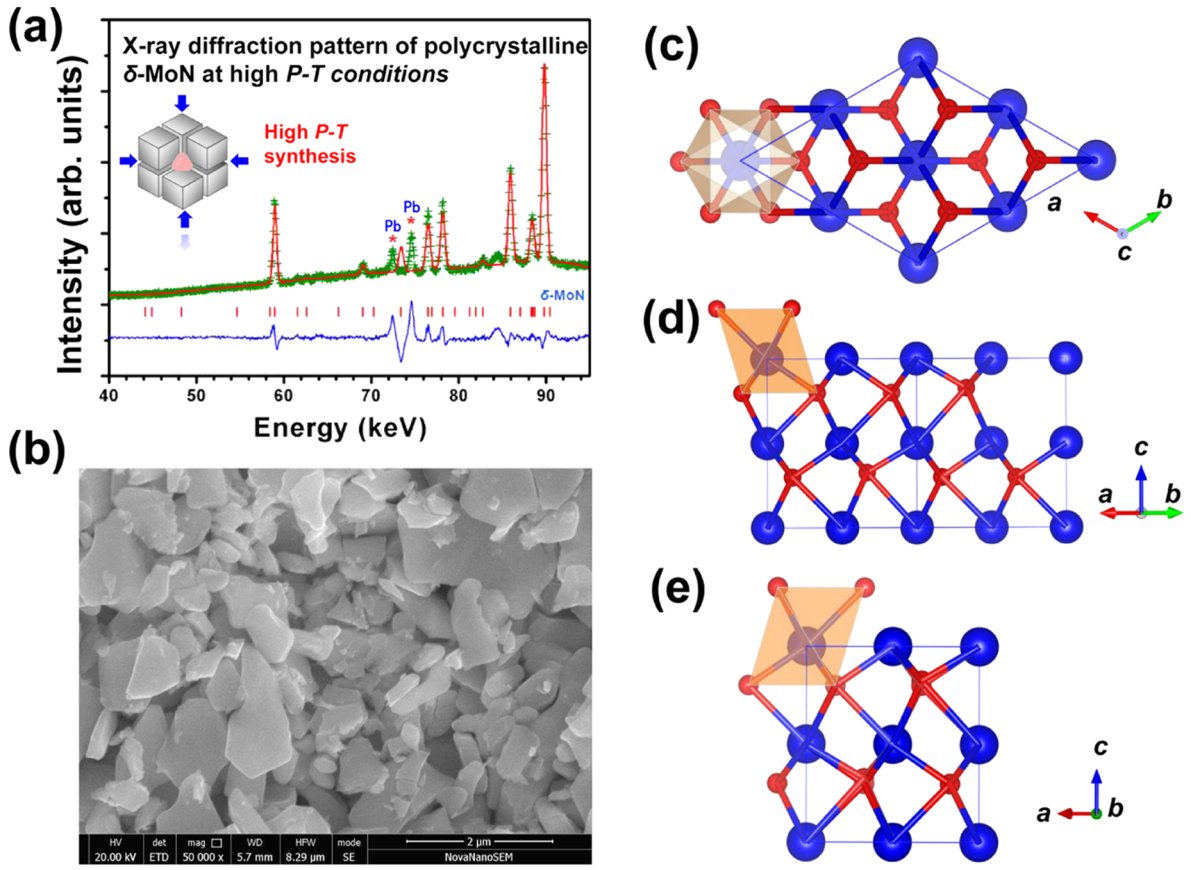

Figure 2. (a) Energy-dispersive X-ray diffraction (XRD) pattern of the synthetic submicron polycrystalline bulk δ-MoN specimen for the present high-pressure ultrasonic measurements, suggesting that the sample is almost a pure phase of δ-MoN without the occurrence of the metastable γ-MoN phase. Lattice parameters and unit-cell volumes of the δ-MoN specimen are refined by the Le Bail method implemented using the EXPGUI/GSAS software package. The solid red curve and green cross represent the Le Bail refined results ($P6_3mc$: no. 186) and observed values, respectively. The bottom blue curve symbolizes the residuals, and the vertical red bars are the peak positions of the δ-MoN phase. The two X-ray peaks marked by red stars are the X-ray fluorescence lines of lead (Pb); (b) SEM image of the high pressure−temperature synthesized polycrystalline δ-MoN bulk specimen for the present ultrasonic velocity measurements. Visible microcracks with an average grain size of ∼0.5 μm are absent in the bulk sample, as estimated by direct SEM observations, exhibiting a homogeneous and equilibrium microstructure. (c−e) Crystal structure of δ-MoN which adopts an unusual hexagonal structure under ambient conditions ($P6_3mc$: no. 186) with a three-dimensional cation−anion network; the Mo atoms are in the octahedrally coordination by the N atoms and the N atoms are trigonally coordinated by the Mo atoms.

performed before calculations. After full optimization, the convergence threshold for the peak pressure/stress is less than ∼0.02 GPa, the self-consistent total energies are converged to $\sim 5.0 \times 10^{-6}$ eV/atom, and the residual force is no more than 0.01 eV/Å. The calculations of total-energy electronic structure are performed using the Cambridge Serial Total Energy Package (CASTEP) code.[36]

RESULTS AND DISCUSSION

A bulk submicron polycrystalline hexagonal δ-MoN specimen used for the current ultrasonic measurements was synthesized at high pressure and high temperature using the as-prepared δ-MoN powders as the starting materials. In situ sound velocity measurements on submicron polycrystalline δ-MoN were performed at pressures of up to ∼13 GPa in a multi-anvil large volume press.

Figure 2a shows Le Bail refinement of energy-dispersive X-ray diffraction patterns of the synthesized δ-MoN bulk specimen used for the current acoustic measurements, indicating that the sintered specimen is almost a pure phase of δ-MoN with a hexagonal structure ($P6_3mc$: no. 186) without the occurrence of the metastable γ-MoN phase which is thermodynamically favorable at temperatures above 1600 °C. To gain insight into the microstructure of the bulk specimen, a representative SEM image is shown in Figure 2b, revealing that in the synthesized specimen, visible microcracks are absent and it exhibits an equilibrium microstructure with an average grain size of about ∼0.5 μm, as estimated by SEM observations. Regarding the structure of δ-MoN shown in Figure 2c−e, the Mo atoms are octahedrally coordinated by N atoms and the N atoms are trigonally coordinated by Mo atoms.

Further chemical composition measurements show that oxygen is absent in our high pressure−temperature synthesized submicron polycrystalline bulk specimen and has a nearly stoichiometric molar ratio of Mo/N = 1:1 from direct SEM-EDX measurements as corrected by the nitride standards, which is identical to the chemical composition of the previously high-pressure synthesized hexagonal δ-MoN specimen.[19] Using Archimedes immersion method, the density of bulk δ-MoN polycrystals yields 9.01(2) g/cm^3, suggesting that our high $P-T$ synthesized specimen exhibits almost a full density of ∼99.6% in terms of the theoretical X-ray density of 9.049 g/cm^3.

Based on the ambient-condition density (ρ_0), initial sample length (L_0), and travel times for both longitudinal (compressional) and transverse (shear) waves (t_p and t_s) under high

https://doi.org/10.1021/acs.inorgchem.1c00406
Inorg. Chem. XXXX, XXX, XXX−XXX

pressure, the high-pressure sample lengths can be easily estimated using the Cook's equation[5,33] as follows

$$\frac{L_0}{L} = 1 + \frac{1 + \alpha\gamma T}{3\rho_0 L_0^2} \int_0^P \frac{dP}{t_P^{-2} - \frac{4}{3}t_s^{-2}} \quad (2)$$

where L, γ, α, and T represent the sample length, Grüneisen parameter, thermal expansivity, and room temperature (~300 K), respectively.

For most materials, it is well accepted that the expansion coefficient (α) and Grüneisen parameter (γ) are in the range of $\alpha = (0.5-3) \times 10^{-5}$ K and $\gamma = 1-2$, respectively. The $\alpha\gamma T$ value is found to be ranging from 0 to 0.02, and its average value is usually assumed to be 0.01,[5,17,20,21,32,33] yielding errors in the sample lengths at various pressures less than ~0.02%, which are within uncertainties. Moreover, we find that no observable sample-length change occurred after our high-pressure acoustic measurement experiments, so it is reasonable to assume that our current static compression experiment is almost purely elastic, and the densities of the bulk specimen upon compression can be derived by the equation[5,37] $\frac{\rho_0}{\rho} = \left(\frac{L}{L_0}\right)^3$.

Based on our obtained travel times and sample-lengths data, the compressional (V_P) and shear (V_S) wave velocities of submicron polycrystalline δ-MoN are derived and plotted as a function of pressure in Figure 3a, as compared with those of our first-principles theoretical calculations. Clearly, both compressional (V_P) and shear (V_S) wave velocities monotonically increase with the increase of pressures up to ~13 GPa without any apparent pressure-induced discontinuity/anomaly in this pressure range. Moreover, we find that the trends in the observed V_P and V_S *vs* pressures are generally consistent with those from our theoretical calculations, especially in the shear wave velocity. A least-square fit of acoustic velocities data at various pressures yields the ambient-condition values of V_P = 7.81(5) km/s and V_S = 4.47(2) km/s, and their pressure dependences, namely $\partial V_P/\partial P$ = 0.148(5) and 0.060(1) km/(m·GPa).

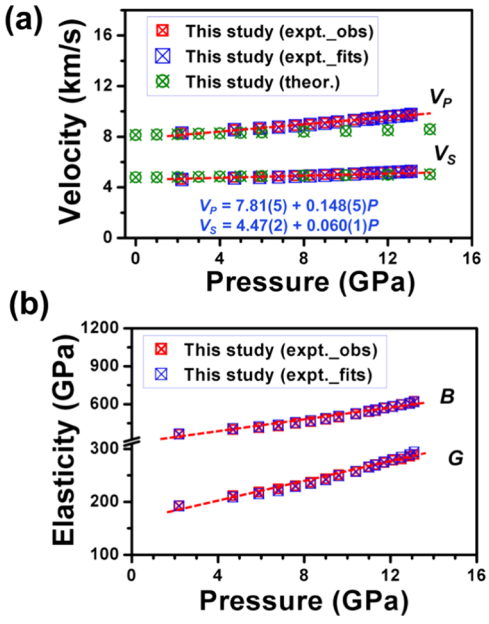

Figure 3. (a) Experimentally observed acoustic compressional (V_P) and shear (V_S) wave velocities of submicron polycrystalline hexagonal δ-MoN at high pressure from the current ultrasonic measurements (in red squares) compared with the fitting results (in blue squares) and those of our DFT theoretical calculations (in green circles). (b) Experimentally observed bulk modulus (B_S) and shear rigidity (G) of polycrystalline hexagonal δ-MoN against pressures from our ultrasonic measurements (in red squares), in comparison with the fitting results (in blue squares). The dashed red lines are guides for the eyes from the least-square fittings of the data of sound velocities and elastic moduli. The errors are within ~0.4% for sound velocities and within ~2% for the bulk modulus and shear rigidity.

Bulk modulus and shear rigidity of hexagonal δ-MoN at high pressure can be calculated from acoustic velocities and densities by applying the equations of $\rho V_P^2 = B_s + 4G/3$ and $\rho V_S^2 = G$. To derive the ambient-pressure bulk modulus and shear rigidity, and their pressure derivatives, the experimental data of sound velocities and densities are fitted to finite-strain equations as follows (eqs 3−8[39])

$$\rho V_P^2 = (1 - 2\varepsilon)^{5/2}(L_1 + L_2\varepsilon) \quad (3)$$

$$\rho V_S^2 = (1 - 2\varepsilon)^{5/2}(M_1 + M_2\varepsilon) \quad (4)$$

$$M_1 = G_0 \quad (5)$$

$$M_2 = 5G_0 - 3B_{S0}G_0' \quad (6)$$

$$L_1 = B_{S0} + 4G_0/3 \quad (7)$$

$$L_2 = 5L_1 - 3B_{S0}(B_{S0}' + 4G_0'/3) \quad (8)$$

where the strain ε is defined as $\varepsilon = [1 - (\rho/\rho_0)^{2/3}]/2$, and the parameters of L_1, L_2, M_1, and M_2 are fitted by the minimum of the difference between the observed and calculated acoustic velocities. On the basis of the fitting results, we can calculate the bulk modulus and shear rigidity (B_{S0} and G_0), and their pressure derivatives of $\partial B_S/\partial P$ and $\partial G/\partial P$, yielding B_{S0} = 360.0(8) GPa, G_0 = 190.0(5) GPa, $\partial B_S/\partial P$ = 3.4(2), and $\partial G/\partial P$ = 1.4(1).

To have an insight into the elastic behavior in compressed δ-MoN, the elasticity of bulk modulus and shear rigidity against pressures are plotted in Figure 3b. Similar to the trends of acoustic velocities *vs* pressures, the bulk and shear moduli of δ-MoN also exhibit a monotonical increase with the increase of pressure, and the shear modulus/rigidity reaches ~278 GPa at ~13 GPa, which is almost as rigid as the cBN composite (~284 GPa).[38]

For good understanding, the ambient-condition bulk and shear moduli of δ-MoN and the corresponding pressure derivatives for our experimental study are shown in Table 1, as compared with those for previous studies on transition-metal mononitrides, as well as our theoretically predicted results. Clearly, our experimentally obtained adiabatic bulk modulus of B_{S0} = 360.0(8) GPa for δ-MoN is generally consistent with its isothermal value of B_{T0} = 345(9) GPa by static compression experiments within the uncertainties,[22] but is ~11% larger than our theoretically predicted result. This difference might have originated from the well-known underbinding of GGA approximation, which usually yields a larger volume and lower compressibility than the experimental value. Clearly seen in Table 1, our obtained bulk modulus of δ-MoN (B_0 = 360 GPa) is comparable to those of hexagonal-structured compounds such as ε-NbN (373.2 GPa),[5] δ-WN (373 GPa),[15] and WC-type TaN (351 GPa),[9] but ~4.3% higher than that (B_0 = 344 GPa) for hexagonal ReN.[12]

https://doi.org/10.1021/acs.inorgchem.1c00406
Inorg. Chem. XXXX, XXX, XXX−XXX

Table 1. Summary of Bulk and Shear Moduli of Hexagonal δ-MoN, as well as Their Pressure Dependences from Our Sound Velocity Measurements and Theoretical Calculations, Compared with Those for Typical Transition-Metal Mononitrides

compounds	B_0 (GPa)	G_0 (GPa)	$\partial B/\partial P$	$\partial G/\partial P$	ref
δ-MoN	360.0(8)	190.0(5)	3.4(2)	1.4(1)	this study (expt.)
δ-MoN	320.5	205.6	3.6	1.7	this study (theor.)
δ-MoN	345(9)		3.5(3)		Soignard et al.[a]
ε-NbN	373.2	200.5	3.81	1.67	Zou et al.[b]
δ-WN	373(8)		4(fixed)		Wang et al.[c]
c-CrN	340, 257		4(fixed)		Rivadulla et al.[d]
					Wang et al.[e]
δ-NbN	319(2)	152	4.4(2)		Tan et al.[f]
WC-type TaN	351(1)		4(fixed)		Yusa et al.[g]
NWCs h-TaN	363(6)		4(fixed)		Gaida et al.[h]
h-ReN	344.4	152.2			Bannikov et al.[i]

[a]Ref 22. [b]Ref 5. [c]Ref 15. [d]Ref 7. [e]Ref 14. [f]Ref 8. [g]Ref 9. [h]Ref 11. [i]Ref 12.

It is noted that the bulk modulus (B_0 = 360 GPa) for polycrstalline δ-MoN is almost the same as that (B_0 = 363 GPa) for a new hexagonal-structured TaN nanowire crystals.[11] When compared with cubic transition-metal mononitrides, we interestingly find that the hexagonal δ-MoN is significantly incompressible than cubic δ-NbN[8] and CrN[7,14] by experimental studies and theoretical prediction. On the other hand, the current experimental shear rigidity of G_0 = 190.0(5) for δ-MoN is comparable to our theoretical result of 205.6 GPa, and the experimental ultrasonic data of ∼200 GPa for hexagonal ε-NbN,[5] but ∼20% lower than the shear modulus for cubic δ-NbN by first-principles calculations.[8] As compared with superhard materials/composites, we find that the hexagonal-structured δ-MoN exhibits a very high bulk modulus, comparable to that of B_0 = 384 GPa for superhard cBN.[24] Its shear rigidity (G_0 = 190.0 GPa) is comparable to that (G_0 = 204 GPa) for the polycrystalline diamond-TiC composite (PCD).[40] It is proposed that the superior elastic/mechanical properties of hexagonal δ-MoN may have originated from the particular σ-band of bonding states between d orbitals for Mo and p orbitals for N, which exhibit a strong resistance of the shear strains.

As shown in Table 1, the pressure dependence of bulk modulus [$\partial B/\partial P$ = 3.4(2)] for δ-MoN from our experimental study is almost identical to our theoretically calculated $\partial B/\partial P$ = 3.6, and the previous compression experiment value[22] of $\partial B/\partial P$ = 3.5(3), but slightly smaller than the previously ultrasonic result of $\partial B/\partial P$ = 3.81 for hexagonal ε-NbN. In terms of the shear rigidity for hexagonal δ-MoN, its pressure dependence of $\partial G/\partial P$ = 1.4(1) from this experimental study is generally consistent with our theoretical values of $\partial G/\partial P$ = 1.7 for hexagonal δ-MoN and $\partial G/\partial P$ = 1.67 for hexagonal ε-NbN,[5] respectively.

It is well accepted that elastic properties of materials are often used to study the strength of interatomic bondings and anharmonicity of lattice vibrations in crystal lattices.[41] To further understand the correlations between sound velocities, elastic moduli, and mechanical/thermal properties of materials, Young's modulus (E), Poisson's ratio (ν), and Grüneisen parameter (γ) are obtained using the following equations[4,20,32,41,42]

$$E = \rho V_S^2(3V_P^2 - 4V_S^2)/(V_P^2 - V_S^2) \quad (9)$$

$$\nu = 0.5(V_P^2 - 2V_S^2)/(V_P^2 - V_S^2) \quad (10)$$

$$\gamma = 1.5[3(V_P/V_S)^2 - 4]/[(V_P/V_S)^2 + 2] \quad (11)$$

It is known that acoustic modes of lattice vibrations are related to acoustic velocities of V_P and V_S. The acoustic Debye temperature (Θ) is usually described as follows

$$\Theta = \left(\frac{h}{k}\right)\left(\frac{3N}{4\pi}\right)^{1/3}\left(\frac{\rho}{M/Z}\right)^{1/3}\left(\frac{1}{3V_P^3} + \frac{2}{3V_S^3}\right)^{(-1/3)} \quad (12)$$

where M, Z, N, k, and h represent the molecular mass, the number of atoms per molecular formula, Avogadro's number, Boltzmann's constant, and Planck's constant, respectively.[4,20,32]

Based on the current measurement data of velocities and densities, the elasticity-related mechanical/thermal properties of Young's modulus (E), Poisson's ratio (ν), Grüneisen parameter (γ), and Debye temperature (Θ) are derived by applying the above eqs 9−12. To well understand the high-pressure behavior of hexagonal polycrystalline δ-MoN under high pressure, the derived elasticity-related mechanical/thermal properties are plotted as a function of pressure in Figure 4a,b. Similar to the trends in sound velocities *vs* pressures, the elasticity-related properties of Young's modulus,

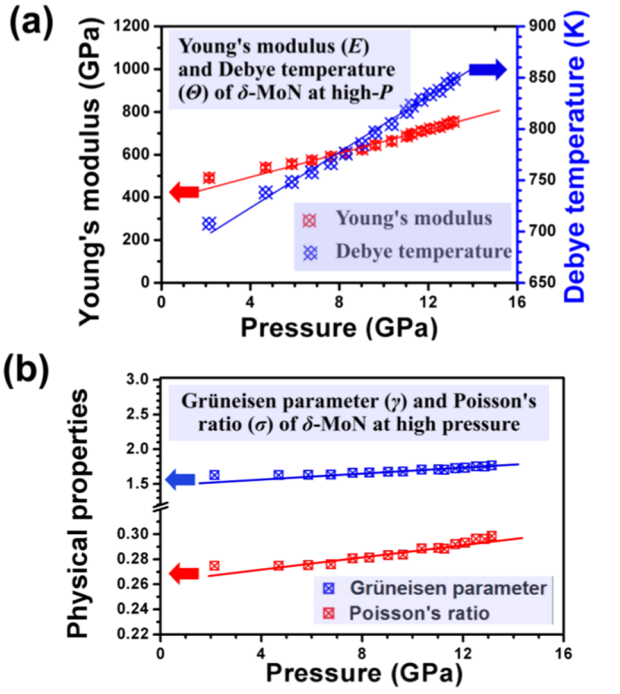

Figure 4. (a) Experimental Young's modulus (E) and Debye temperature (Θ) of hexagonal submicron polycrystalline δ-MoN *vs* pressure from our ultrasonic measurements; (b) Experimental Grüneisen parameter (γ) and Poisson's ratio (ν) of δ-MoN against pressures. The solid lines are from the least-squares fittings of the elasticity-correlated mechanical/thermal properties using a linear function of pressure. The associated errors are within 2−3%.

https://doi.org/10.1021/acs.inorgchem.1c00406
Inorg. Chem. XXXX, XXX, XXX−XXX

Table 2. Summary of Bulk Modulus (B), Shear Rigidity (G), Young's Modulus (E), Debye Temperature (Θ), Poisson's Ratio (ν), Grüneisen Parameter (γ), Vickers Hardness (H_v), and Fracture Toughness (K_{IC}) of Submicron Polycrystalline δ-MoN, in Comparison with Those for Other Nitrides and Superhard/High-Hard Materials

compounds	B (GPa)	G (GPa)	E (GPa)	B/G	Θ (K)	ν	γ	H_v (GPa)	K_{IC} (MPa·m$^{1/2}$)	ref
δ-MoN	360.0	190.0	484.7	1.89	683	0.28	1.53	17.4	4.3	this study
ε-NbN	373.2	200.5	510	1.86	738	0.27	1.53	18.5		Zou et al.[a]
cBN	384	406		0.95				75	5	Liu et al.[b] and Young[b]
PcBN	254	284		0.89				36		Novikov and Dub[c]
PDC	183	204	446	0.90				45		Wang et al.[d]
δ-WN	376.7	149.2	395.4	2.52		0.32	1.53	13.8		Wang et al.[e]
γ-B	214	227	503	0.94				30.3	3.0,[g] 4.1[h]	Qin et al.[f]

[a]Ref 5. [b]Refs 24 and 45. [c]Ref 38. [d]Ref 40. [e]Refs 6 and 15. [f]Ref 43. [g]Calculated value using the empirical model. [h]Experimental value.

Poisson's ratio, Grüneisen parameter, and Debye temperature (seen in Figure 4a,b), exhibit a monotonic increase with the increase of pressures up to ~13 GPa without the occurrence of any observable pressure-induced discontinuity during compression. Least-square fittings of the elasticity-related properties at various pressures, we obtain the ambient-condition values of Young's modulus, Poisson's ratio, Grüneisen parameter, and Debye temperature, as summarized in Table 2.

Interestingly, hexagonal δ-MoN possesses superior incompressibility, which is almost as incompressible as superhard cBN with B_0 = 384 GPa,[24] and is also comparable to the hexagonal δ-WN (~395 GPa).[15] The shear rigidity of δ-MoN (~190 GPa) is comparable to those of superhard diamond-TiC composites (PDC: ~204 GPa),[40] hexagonal ε-NbN (~200.5 GPa),[5] and superhard/hard γ-B (227 GPa).[43] Similarly, our experimentally obtained Young's modulus of E = 484.7 GPa for δ-MoN is comparable to those of materials with high hardness ε-NbN[5] and γ-B,[43] but surpasses those of superhard PDC (~446 GPa)[40] and hexagonal δ-WN (~395 GPa).[15]

In addition to the bulk modulus, shear rigidity, and Young's modulus, our obtained ambient-condition value of Poisson's ratio of ν = 0.28 is found to be in excellent agreement with the theoretical value (ν = 0.28) for δ-MoN by Kanoun et al.,[23] but slightly smaller than that (ν = 0.32) for hexagonal δ-WN.[15] The current ambient-condition Grüneisen parameter of γ = 1.53 is almost the same as γ = 1.51 for δ-MoN,[12] and γ = 1.53 for hexagonal ε-NbN and δ-WN by theoretical calculations.[5,15] By contrast, the current experimental value of Debye temperature for δ-MoN is determined to be Θ = 683 K, which is 8−9% lower than the theoretical result of Θ = 747 K.[12] Furthermore, the Pugh's modulus ratio is defined as $k = B/G$, namely the ratio of bulk modulus to shear rigidity, is often applied to predict the ductility and/or brittleness of materials.[31] If k > 1.75, materials usually have a ductile behavior, otherwise, they adopt a brittle one.[31] In the case of submicron polycrystalline δ-MoN, our experimentally obtained Pugh's modulus ratio ($k = B/G$) is determined to be k = 1.89, which is almost the same as that of the hexagonal ε-NbN,[5] but higher than those of cBN (k = 0.95), polycrystalline cBN (PcBN) (k = 0.89), and γ-B (k = 0.94), indicating that the submicron δ-MoN polycrystals exhibit a much ductile behavior compared with some representative hard/superhard materials in Table 2.

According to thermodynamic equations and Gilvarry's rule,[44] the melting temperature (T_m) of materials at various pressures can be described as $T_m = AV^{2/3}\Theta^2$, in which A is a constant and can be determined from the zero-pressure melting point of T_m = 2023 K for δ-MoN. It is found that this equation is similar to the Lindemann melting criterion.[45] On the basis of the equation mentioned above, the melting temperature curve of δ-MoN against pressures can be calculated, as shown in Figure S1c of the Supporting Information.[46] A linear fitting of T_m as a function of pressure yields the equation $T_m = 58.9P + 2011.5$ K. As shown in Figure S1c, we find that T_m is monotonically increasing with an increase in pressure.

With regard to hardness, it is one of the important physical properties of hard/superhard materials for mechanical applications. To gain further insights into the correlations between elasticity of bulk modulus, shear rigidity, and hardness, an empirical formula of Vickers hardness is estimated as $H_v = 2(k^{-2}G)^{0.585} - 3$ (in GPa), where k is the ratio of the bulk modulus (B) to shear rigidity (G).[47] Using this hardness model and our obtained elasticity data, the Vickers hardness of submicron δ-MoN is estimated to be ~17.4 GPa. As clearly seen in Table 2 and Figure S1a in the Supporting Information,[46] the hexagonal submicron polycrystalline δ-MoN is not so hard as previously reported by Wang et al.[19] We find that this nitride is almost as hard as hexagonal ε-NbN[5] (H_v = ~18.5 GPa), but is ~21% harder than the hexagonal δ-WN (H_v = 13.8 GPa) by direct experimental Vickers hardness measurements,[15] and significantly softer than those of other superhard/hard materials, such as cBN,[24] PcBN,[38] PCD,[40] and γ-B.[43]

Similar to hardness, fracture toughness (K_{IC}) is also an important parameter for mechanical applications, and means the resistance of materials against crack propagations. According to the empirical model,[29,48] fracture toughness of covalent and ionic crystals can be calculated by the equation as expressed below

$$K_{IC} = V_0^{1/6} \cdot G \cdot \left(\frac{B}{G}\right)^{1/2} \tag{13}$$

where the unit of K_{IC} is MPa·m$^{1/2}$, V_0 is the volume per atom (in m^3); B and G are the bulk modulus and shear rigidity (in MPa), respectively.

To test the validation of the model mentioned above, we have calculated the fracture toughness of superhard cBN, yielding $K_{IC} \approx 5.4$ MPa·m$^{1/2}$, which agrees well with the direct experimental value of 5.0 MPa·m$^{1/2}$.[29] In terms of hexagonal submicron polycrystalline δ-MoN, the fracture toughness of δ-MoN is determined to be ~4.3 MPa·m$^{1/2}$ by applying the empirical model,[29] which is almost the same value as that of superhard/hard γ-B,[43] and is also comparable to those for diamond (4−7 MPa·m$^{1/2}$),[49] cBN (2−5 MPa·m$^{1/2}$),[50] and TiN (3.4−5 MPa·m$^{1/2}$),[51] respectively. Assuming that eq 13 is also

https://doi.org/10.1021/acs.inorgchem.1c00406
Inorg. Chem. XXXX, XXX, XXX−XXX

suitable for materials upon compression, the fracture toughness of δ-MoN is plotted as a function of pressure, as shown in Figure S1b of the Supporting Information.[46] Clearly, the fracture toughness is monotonically increasing with the increase of pressure, exhibiting an obvious work hardening behavior under high pressure.

To further understand the underlying mechanism of the unique mechanical properties of hexagonal δ-MoN, the bulk modulus (B_0), shear rigidity/modulus (G_0), and Vickers hardness (H_v) are plotted as a function of ambient-condition volume per atom, as compared with those for the isostructured NaCl-type cubic γ-MoN, δ-NbN, δ-ZrN,[3,12,19,23] and hexagonal ε-NbN[5] in Figure 5a−c. It is known that the hexagonal

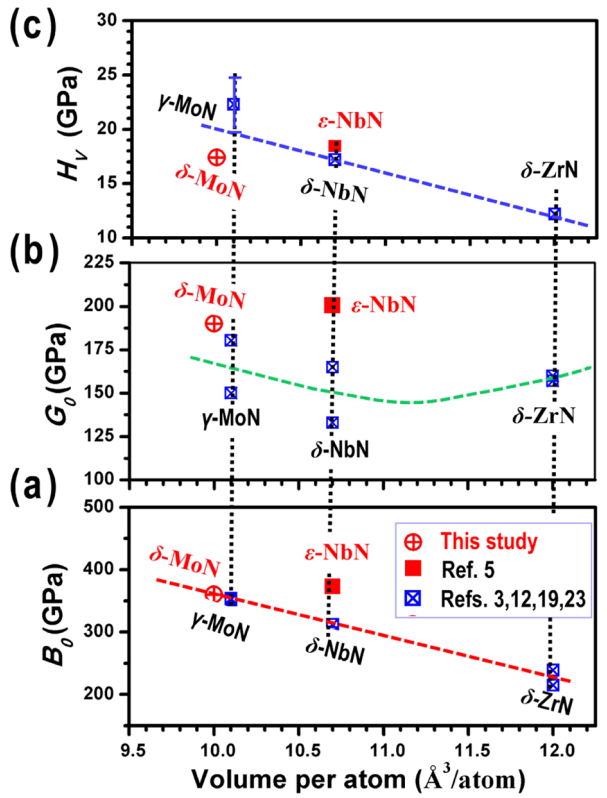

Figure 5. Bulk modulus (a), shear modulus (b) and Vickers hardness (c) as a function of volume per atom for hexagonal δ-MoN, in comparison with those for nearest-neighbor transition-metal nitrides with a cubic NaCl structure (*i.e.*, δ-NbN, δ-ZrN, γ-MoN)[3,12,19,23] and hexagonal ε-NbN.[5]

δ-MoN is a low-density structure/phase, which is about 9.5% less dense than the cubic γ-MoN sample.[19] As clearly seen in Figure 5a, the low-density phase of hexagonal δ-MoN possesses a strong bulk modulus of B_0 = 360.0 GPa, which has almost the same value as B_0 = 351.6 GPa for stoichiometric cubic γ-MoN by ab initio theoretical calculations,[23] but ∼9% higher than that ($B_0 \approx$ 302 GPa) for unstoichiometric cubic γ-$MoN_{0.86}$.[19] The reason for this elastic softening in cubic γ-$MoN_{0.86}$ is probably ascribed to nitrogen vacancies in the cubic structure. Because of the nitrogen vacancy in the unstoichiometric transition-metal nitrides, the anion−cation covalent p−d bonds become soft. In comparison with the metallic d−d bonds, the fraction of these p−d metallic bonds are increased owing to the unstoichiometry or nitrogen vacancy, which results in elastic softening in these compounds. In terms of shear modulus, our experimentally obtained G_0 = 190 GPa for δ-MoN is significantly larger than the previously reported values of 150−180 GPa for the high-density cubic γ-MoN.[3,12,23] This anomalous shear strengthening in δ-MoN, as compared with cubic γ-MoN, is probably attributed to the three-dimensional covalent bonding network in the hexagonal structure.

As shown in Figure 5c, our recently obtained experimental Vickers hardness of ∼18.5 for hexagonal ε-NbN[4,5] is slightly larger that for δ-NbN (∼17.2 GPa).[23] For hexagonal δ-MoN, however, our obtained H_v = 17.4 GPa is significantly lower than those for γ-MoN ($H_v \approx$ 23 GPa) and for δ-MoN ($H_v \approx$ 30 GPa) at relatively low loading of ∼0.5 N.[19] This discrepancy might be due to the low loads and the absence of asymptotic hardness values.

Comparison of the nearest-neighbor NaCl-structured transition-metal nitrides (*i.e.*, δ-NbN, δ-ZrN) in Figure 5a−c, the bulk modulus (B_0) *vs* volume-per-volume exhibits a linear behavior and decreases with the increase in volume-per-atom. As shown in Figure 5c, it seems that the Vickers hardness (H_v) increases with the decreasing volume-per-atom for the cubic nitrides, which is significantly different from the behavior of shear modulus (G). We propose that the shortened cation−anion distance in the high-density phase of γ-MoN may be responsible for its high hardness, as compared with the near-neighbor cubic transition-metal nitrides, such as δ-NbN and δ-ZrN.

It is well accepted that the electronic structures and bonding nature are important properties to understand the structural stability and the origin of hardness and elasticity of materials.[1,15,52] To gain deeper insights into the changes in the electronic structures, the total and partial density of states (DOS) of hexagonal δ-MoN at 0 GPa are shown in Figure 6a, as compared with those at a pressure of 10 GPa.

As shown in Figure 6a, it is found that the Fermi level (E_F) continuously crosses in some energy bands, indicating that the hexagonal δ-MoN exhibits metallic behavior. The total and partial DOS profiles near the E_F show sharp peaks, which have mainly originated from the d state of Mo atoms and are responsible for the metallic behavior between Mo−Mo atoms. As a result, the Mo−Mo metallic bond may lead to weakening/softening of the elasticity and hardness of hexagonal δ-MoN. Clearly, Figure 6a shows a strong hybridization between the 2p state of N and the 4d state of Mo in hexagonal δ-MoN with the occurrence of a pseudogap above E_F, which indicates no covalent hybridization between N and Mo atoms. Similar to hexagonal δ-WN,[15] electric charge transfer from W to N atoms may also occur in δ-MoN, indicating ionic behavior of Mo−N bonds. As proposed by Wang et al.,[15] ionic bonds do not contribute to high hardness, but covalent bonds can resist plastic deformation and restrain the formation/propagation of defects, resulting in the enhancement of the hardness of materials. For hexagonal δ-MoN, the absence of covalent bonds between Mo and N atoms results in an easy deformation in the hexagonal structure under shear stress, eventually lowering the hardness (∼17.4 GPa) of δ-MoN.

On the other hand, the total DOS for δ-MoN at 0 GPa around E_F lies in a dip. It increases monotonically at E_F with the increase of pressures up to 10 GPa (in Figure 6a,b), indicating that hexagonal δ-MoN becomes dynamically unstable under high pressure, which agrees with the total-energy calculation results. As shown in Figure 6a,b, the upper region of the valence-bands is separated by E_F, mainly owing to the 4d states of Mo mixed with the 2p states of N. Clearly, the

https://doi.org/10.1021/acs.inorgchem.1c00406
Inorg. Chem. XXXX, XXX, XXX−XXX

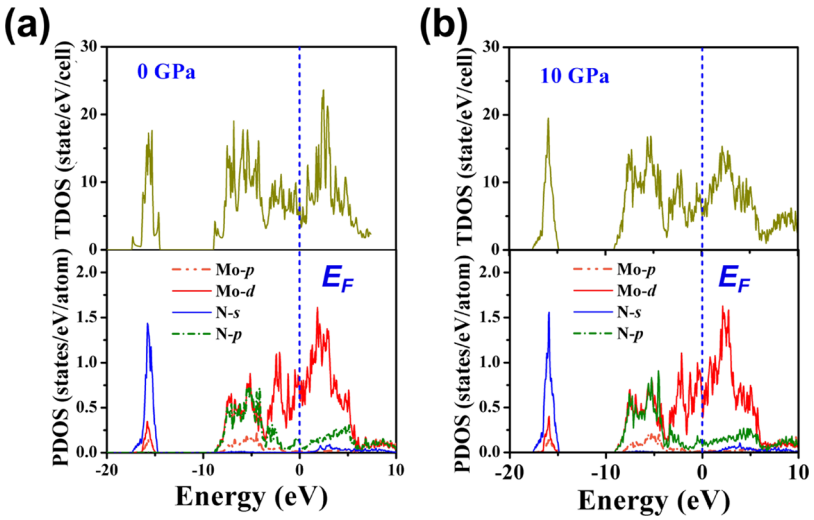

Figure 6. (a) Total and partial density of states (DOS) of hexagonal δ-MoN at 0 GPa, in comparison with those at 10 GPa (b). Blue vertical-dashed lines denote the Fermi level (E_F).

2p states of N are strongly hybridized by the 4d states of Mo, and the energy region above E_F is mainly owing to the unoccupied 4d states of Mo atoms. Thus, we propose that the origin of the electronic structure of δ-MoN is attributed to the expanded hexagonal lattices owing to the inserted nitrogen atoms in the trigonal prismatic sites and the interaction between the 2p electrons of N and 4d electrons of Mo.

CONCLUSIONS

In summary, acoustic velocities, elasticity, and elasticity-correlated mechanical/thermal properties of stoichiometric submicron polycrystalline δ-MoN have been studied at high pressure in a multi-anvil press, complemented with first-principles calculations. On the basis of the experimental data of sound velocities and densities, we obtain the bulk modulus and shear rigidity, the associated pressure derivatives, and other elasticity-related mechanical/thermal properties such as Grüneisen parameter, Debye temperature, Poisson's ratio, hardness, and fracture toughness. It is interesting to find that the hexagonal δ-MoN is almost as incompressible as superhard cBN and ε-NbN. Moreover, the shear rigidity (~190 GPa) of δ-MoN is found to be comparable to those of superhard diamond-TiC composite (PDC: ~204 GPa) and hexagonal ε-NbN (~200 GPa). Using Chen's model,[28] the Vickers hardness of polycrystalline δ-MoN is estimated to be ~17.4 GPa, which is almost as hard as hexagonal ε-NbN.[5] The fracture toughness of δ-MoN is determined to be ~4.3 MPa·$m^{1/2}$, which is almost the same value as that of superhard/hard γ-B,[43] and is comparable to those of diamond (4–7 MPa·$m^{1/2}$),[49] cBN (2–5 MPa·$m^{1/2}$),[50] and TiN (3.4–5 MPa·$m^{1/2}$),[51] respectively. These new results may be very important for the technological and engineering applications of δ-MoN under extreme conditions.

ASSOCIATED CONTENT

Supporting Information

The Supporting Information is available free of charge at https://pubs.acs.org/doi/10.1021/acs.inorgchem.1c00406.

SEM image of the rough surface of bulk δ-MoN; melting temperature and fracture toughness *vs* pressures; hardness; experimental results for polycrystalline δ-MoN at high pressure (PDF)

AUTHOR INFORMATION

Corresponding Authors

Yongtao Zou − *Shenzhen Key Laboratory of Ultraintense Laser and Advanced Material Technology, and College of Engineering Physics, Shenzhen Technology University, Shenzhen 518118, China; United Laboratory of High-Pressure Physics and Earthquake Science, Institute of Earthquake Science, China Earthquake Administration, Beijing 100036, China;* orcid.org/0000-0001-8725-9418; Email: zouyongtao@sztu.edu.cn

Leiming Fang − *Key Laboratory for Neutron Physics, Institute of Nuclear Physics and Chemistry, China Academy of Engineering Physics, Mianyang 621900, China*; Email: flmyaya2008@163.com

Shuangchen Ruan − *Shenzhen Key Laboratory of Ultraintense Laser and Advanced Material Technology, and College of Engineering Physics, Shenzhen Technology University, Shenzhen 518118, China*; Email: scruan@sztu.edu.cn

Cangtao Zhou − *Shenzhen Key Laboratory of Ultraintense Laser and Advanced Material Technology, and College of Engineering Physics, Shenzhen Technology University, Shenzhen 518118, China*; Email: zcangtao@sztu.edu.cn

Authors

Ke Liu − *College of Physics and Electronic Engineering, Sichuan Normal University, Chengdu 610101, China*

Pei Wang − *Academy for Advanced Interdisciplinary Studies and Department of Physics, Southern University of Science and Technology (SUSTech), Shenzhen 518055, China;* orcid.org/0000-0002-0423-9639

Daowei Wang − *Shenzhen Key Laboratory of Ultraintense Laser and Advanced Material Technology, and College of Engineering Physics, Shenzhen Technology University, Shenzhen 518118, China*

Mu Li − *Shenzhen Key Laboratory of Ultraintense Laser and Advanced Material Technology, and College of Engineering Physics, Shenzhen Technology University, Shenzhen 518118, China*

https://doi.org/10.1021/acs.inorgchem.1c00406
Inorg. Chem. XXXX, XXX, XXX−XXX

Ying Li − *United Laboratory of High-Pressure Physics and Earthquake Science, Institute of Earthquake Science, China Earthquake Administration, Beijing 100036, China*
Hongbin Zhuo − *Shenzhen Key Laboratory of Ultraintense Laser and Advanced Material Technology, and College of Engineering Physics, Shenzhen Technology University, Shenzhen 518118, China*
Yusheng Zhao − *Academy for Advanced Interdisciplinary Studies and Department of Physics, Southern University of Science and Technology (SUSTech), Shenzhen 518055, China*

Complete contact information is available at: https://pubs.acs.org/10.1021/acs.inorgchem.1c00406

Author Contributions

The manuscript was written through contributions from all authors. All authors have given approval to the final version of the manuscript.

Notes

The authors declare no competing financial interest.

■ ACKNOWLEDGMENTS

This work was supported by the National Natural Science Foundation of China (nos. 11872198, U2030110, 52002166, 11772310, 11974321, and 11972330), the Shenzhen Fundamental Research Program, China (no. JCYJ20190813103201662), the Key Research Platforms and Research Projects of Universities in Guangdong Province, China (no. 2020ZDZX2035), the Natural Science Foundation of Top Talent of Shenzhen Technology University (SZTU), China (no. 2019202), and partially supported by the Science Challenge Project (no. TZ2016001). We also thank the crew of SGII laser facility for their helpful support.

■ REFERENCES

(1) Jhi, S. H.; Ihm, J.; Louie, S. G.; Cohen, M. L. Electronic Mechanism of Hardness Enhancement in Transition-Metal Carbonitrides. *Nature* **1999**, *399*, 132−134.
(2) Friedrich, A.; Winkler, B.; Bayarjargal, L.; Morgenroth, W.; Juarez-Arellano, E. A.; Milman, V.; Refson, K.; Kunz, M.; Chen, K. Novel Rhenium Nitrides. *Phys. Rev. Lett.* **2010**, *105*, No. 085504.
(3) Wu, Z. G.; Chen, X. J.; Struzhkin, V. V.; Cohen, R. E. Trends in Elasticity and Electronic Structure of Transition-Metal Nitrides and Carbides from First Principles. *Phys. Rev. B* **2005**, *71*, No. 214103.
(4) Zou, Y.; Qi, X.; Zhang, C.; Ma, S.; Zhang, W.; Li, Y.; Chen, T.; Wang, X.; Chen, Z.; Welch, D.; Zhu, P.; Liu, B. B.; Li, Q.; Cui, T.; Li, B. Discovery of Superconductivity in Hard Hexagonal ε-NbN. *Sci. Rep.* **2016**, *6*, No. 22330.
(5) Zou, Y.; Wang, X.; Chen, T.; Li, X.; Qi, X.; Welch, D.; Zhu, P.; Liu, B. B.; Cui, T.; Li, B. Hexagonal-structured ε-NbN: Ultra-incompressibility, High Shear Rigidity, and a Possible Hard Superconducting Material. *Sci. Rep.* **2015**, *5*, No. 10811.
(6) McMillan, P. F. New Materials from High-Pressure Experiments. *Nat. Mater.* **2002**, *1*, 19−25.
(7) Rivadulla, F.; Bañobre-López, M.; Quintela, C. X.; Piñeiro, A.; Pardo, V.; Baldomir, D.; López-Quintela, M. A.; Rivas, J.; Ramos, C. A.; Salva, H.; Zhou, J.-S.; Goodenough, J. B. Reduction of the Bulk Modulus at High Pressure in CrN. *Nat. Mater.* **2009**, *8*, 947−951.
(8) Tan, J.; Zhang, S.; Wang, S.; Wang, W.; Zheng, X.; Zhao, J.; Li, W.; Mao, X.; Liu, K.; Zhou, X.; Zhao, Y.; Jin, C. Q.; Yu, X. Stoichiometric δ-NbN: The Most Incompressible Cubic Transition metal Mononitride. *Phys. Status Solidi B* **2017**, *254*, No. 1700063.
(9) Yusa, H.; Kawamura, F.; Taniguchi, T.; Hirao, N.; Ohishi, Y.; Kikegawa, T. High-Pressure Synthesis and Compressive Behavior of Tantalum Nitrides. *J. Appl. Phys.* **2014**, *115*, No. 103520.
(10) Holec, D.; Friák, M.; Neugebauer, J.; Mayrhofer, P. H. Trends in the Elastic Response of Binary Early Transition Metal Nitrides. *Phys. Rev. B* **2012**, *85*, No. 064102.
(11) Gaida, N. A.; Sasaki, T.; Liu, Z.; Niwa, K.; Hirozawa, M.; Ohsuna, T.; Hasegawa, M. Nanowire Crystals of Tantalum Nitride Grown in Ammonium Halide Fluxes at High Pressures,. *Appl. Phys. Lett.* **2020**, *116*, No. 123102.
(12) (a) Zhao, E.; Wang, J.; Wu, Z. Displacive Phase Transition, Structural Stability, and Mechanical Properties of the Ultra-incompressible and Hard MoN by First Principles. *Phys. Status Solidi B* **2010**, *247*, 1207−1213. (b) Bannikov, V. V.; Shein, I. R.; Ivanovskii, A. L. Elastic and Electronic Properties of Hexagonal Rhenium Sub-nitrides Re_3N and Re_2N In Comparison With *hcp*-Re and Wurtzite-Like Rhenium Mononitride ReN. *Phys. Status Solidi B* **2011**, *248*, 1369−1374.
(13) Kral, C.; Lengauer, W.; Rafaja, D.; Ettmayer, P. Critical Review on the Elastic Properties of Transition Metal Carbides, Nitrides and Carbonitrides. *J. Alloys Compd.* **1998**, *265*, 215−233.
(14) Wang, S.; Yu, X.; Zhang, J.; Chen, M.; Zhu, J.; Wang, L.; He, D.; Lin, Z.; Zhang, R.; Leinenweber, K.; Zhao, Y. Experimental Invalidation of Phase-Transition-Induced Elastic Softening in CrN. *Phys. Rev. B* **2012**, *86*, No. 064111.
(15) Wang, C.; Tao, Q.; Dong, S.; Wang, X.; Zhu, P. Synthesis and Mechanical Character of Hexagonal Phase δ-WN. *Inorg. Chem.* **2017**, *56*, 3970−3975.
(16) Bull, C. L.; McMillan, P. F.; Soignard, E.; Leinenweber, K. Determination of the Crystal Structure of δ-MoN by Neutron Diffraction. *J. Solid State Chem.* **2004**, *177*, 1488−1492.
(17) Liu, K.; Dong, B.; Zhou, X.; Wang, S.; Zhao, Y.; Chang, J. Structural, Elastic, and Thermodynamic Properties of Hexagonal Molybdenum Nitrides under High Pressure from First Principles. *J. Alloys Compd.* **2015**, *632*, 830−836.
(18) Yang, Z.-X.; Kuang, X.-Y.; Wang, Z.; Zhong, M.; Huang, X. The Mechanical Properties of MoN under High Pressure and Effect of Metallic Bonding on Its Hardness. *Solid State Sci.* **2014**, *28*, 20−25.
(19) Wang, S.; Antonio, D.; Yu, X.; Zhang, J.; Cornelius, A. L.; He, D.; Zhao, Y. The Hardest Superconducting Metal Nitride. *Sci. Rep.* **2015**, *5*, No. 13733.
(20) Zou, Y.; Li, Y.; Chen, H.; Welch, D.; Zhao, Y.; Li, B. Thermoelasticity and Anomalies in the Pressure Dependence of Phonon Velocities in Niobium. *Appl. Phys. Lett.* **2018**, *112*, No. 011901.
(21) Liu, W.; Zeng, Q.; Jiang, Q.; Wang, L.; Li, B. Density and Elasticity of $Zr_{46}Cu_{37.6}Ag_{8.4}Al_8$ Bulk Metallic Glass at High Pressure. *Scr. Mater.* **2011**, *65*, 497.
(22) Soignard, E.; Shebanova, O.; McMillan, P. F. Compressibility Measurements and Phonon Spectra of Hexagonal Transition-Metal Nitrides at High Pressure: ε-TaN, δ-MoN, and Cr_2N. *Phys. Rev. B* **2007**, *75*, No. 014104.
(23) (a) Kanoun, M. B.; Goumri-Said, S.; Jaouen, M. Structure and Mechanical Stability of Molybdenum Nitrides: A First-Principles Study. *Phys. Rev. B* **2007**, *76*, No. 134109. (b) Fulcher, B. D.; Cui, X. Y.; Delley, B.; Stampfl, C. Hardness Analysis of Cubic Metal Mononitrides from First Principles. *Phys. Rev. B* **2012**, *85*, No. 184106. (c) Chen, X.-J.; Struzhkin, V. V.; Wu, Z.; Somayazulu, M.; Qian, J.; Kung, S.; Christensen, A. N.; Zhao, Y.; Cohen, R. E.; Mao, H.-K.; Hemley, R. J. Hard Superconducting Nitrides. *Proc. Natl. Acad. Sci. U.S.A.* **2005**, *102*, 3198.
(24) Liu, G.; Kou, Z.; Yan, X.; Lei, L.; Peng, F.; Wang, Q.; Wang, K.; Wang, P.; Li, L.; Li, Y.; Li, W.; Wang, Y.; Bi, Y.; Leng, Y.; He, D. Submicron Cubic Boron Nitride As Hard As Diamond. *Appl. Phys. Lett.* **2015**, *106*, No. 121901.
(25) Zhao, Y.; Qian, J.; Daemen, L. L.; Pantea, C.; Zhang, J.; Voronin, G. A.; Zerda, T. W. Enhancement of Fracture Toughness in Nanostructured Diamond-SiC Composites. *Appl. Phys. Lett.* **2004**, *84*, 1356.
(26) Brazhkin, V.; Dubrovinskaia, N.; Nicol, M.; Novikov, N.; Riedel, R.; Solozhenko, V.; Zhao, Y. What Does 'Harder Than Diamond' Mean? *Nat. Mater.* **2004**, *3*, 576−577.

(27) Jiang, X.; Zhao, J.; Jiang, X. Correlation Between Hardness and Elastic Moduli of the Covalent Crystals. *Comput. Mater. Sci.* **2011**, *50*, 2287−2290.
(28) Chen, X.-Q.; Niu, H.; Franchini, C.; Li, D.; Li, Y. Hardness of *T*-Carbon: Density Functional Theory Calculations. *Phys. Rev. B* **2011**, *84*, No. 121405(R).
(29) Niu, H.; Niu, S.; Oganov, A. R. Simple and Accurate Model of Fracture Toughness of Solids. *J. Appl. Phys.* **2019**, *125*, No. 065105.
(30) Sanditov, D. S.; Darmaev, M. V.; Sanditov, B. D.; Mantatov, V. V. Grüneisen Parameter and Velocities of Propagation of Sound Waves in Rigid Bodies. *Russ. Phys. J.* **2009**, *52*, 386−389.
(31) Pugh, S. F. Relations Between the Elastic Moduli and the Plastic Properties of Polycrystalline Pure Metals. *London, Edinburgh Dublin Philos. Mag. J. Sci.* **1954**, *45*, 823.
(32) Zou, Y.; Zhang, W.; Chen, T.; Li, X.; Wang, C.-H.; Qi, X.; Wang, S.; Yu, T.; Liu, B. B.; Wang, Y.; Liebermann, R. C.; Zhao, Y.; Li, B. Thermally Induced Anomaly in the Shear Behavior of Magnetite at High Pressure. *Phys. Rev. Appl.* **2018**, *10*, No. 024009.
(33) (a) Wang, X.; Chen, T.; Qi, X.; Zou, Y.; Kung, J.; Yu, T.; Wang, Y.; Liebermann, R. C.; Li, B. Acoustic Travel Time Gauges for In-Situ Determination of Pressure and Temperature in Multi-Anvil Apparatus. *J. Appl. Phys.* **2015**, *118*, No. 065901. (b) Cook, R. K. Variation of Elastic Constants and Static Strains with Hydrostatic Pressure: A Method for Calculation from Ultrasonic Measurements. *J. Acoust. Soc. Am.* **1957**, *29*, 445.
(34) Vanderbilt, D. Soft Self-consistent Pseudopotentials in a Generalized Eigenvalue Formalism. *Phys. Rev. B* **1990**, *41*, 7892.
(35) Perdew, J. P.; Burke, K.; Ernzerhof, M. Generalized Gradient Approximation Made Simple. *Phys. Rev. Lett.* **1996**, *77*, 3865.
(36) Segall, M. D.; Lindan, P. J. D.; Probert, M. J.; Pickard, C. J.; Hasnip, P. J.; Clark, S. J.; Payne, M. C. First-Principles Simulation: Ideas, Illustrations and the CASTEP Code. *J. Phys.: Condens. Matter.* **2002**, *14*, 2717−2744.
(37) Chen, T.; Gwanmesia, G. D.; Wang, X.; Zou, Y.; Liebermann, R. C.; Michaut, C.; Li, B. Anomalous Elastic Properties of Coesite at High Pressure and Implications for the Upper Mantle X-discontinuity. *Earth Planet. Sci. Lett.* **2015**, *412*, 42.
(38) Davies, G.; Dziewonski, A. Homogeneity and Constitution of the Earth's Lower Mantle and Outer Core. *Phys. Earth Planet. Inter.* **1975**, *10*, 336−343.
(39) Novikov, N. V.; Dub, S. N. Fracture Toughness of Diamond Single Crystals. *J. Hard Mater.* **1991**, *2*, 3−11.
(40) Wang, H.; He, D.; Xu, C.; Tang, M.; Li, Y.; Dong, H.; Meng, C.; Wang, Z.; Zhu, W. Nanostructured Diamond-TiC Composites with High Fracture Toughness. *J. Appl. Phys.* **2013**, *113*, No. 043505.
(41) Jacobsen, M. K.; Velisavljevic, N.; Kono, Y.; Park, C.; Kenney-Benson, C. Shear-driven Instability in Zirconium at High Pressure and Temperature and Its Relationship to Phase-boundary Behaviors. *Phys. Rev. B* **2017**, *95*, No. 134101.
(42) Sanditov, D. S.; Belomestnykh, V. N. Relation between the Parameters of the Elasticity Theory and Averaged Bulk Modulus of Solids. *Tech. Phys.* **2011**, *56*, 1619−1623.
(43) Qin, J.; Nishiyama, N.; Ohfujia, H.; Shinmei, T.; Lei, L.; He, D.; Irifune, T. Polycrystalline γ-boron: As Hard As Polycrystalline Cubic Boron Nitride. *Scr. Mater.* **2012**, *67*, 257−260.
(44) Gilvarry, J. J. The Lindemann and Grüneisen Laws. *Phys. Rev.* **1956**, *102*, 308−316.
(45) Young, D. A. *Phase Diagram of the Elements*, University California Press, 1991.
(46) See Supporting Information for the experimental results of the changes of elastic-related physical properties of submicron polycrystalline δ-MoN under high pressure, such as melting temperature curve, hardness and fracture toughness.
(47) Chen, X.-Q.; Niu, H.; Li, D.; Li, Y. Modeling Hardness of Polycrystalline Materials and Bulk Metallic Glasses. *Intermetallics* **2011**, *19*, 1275−1281.
(48) Kvashnin, A. G.; Allahyari, Z.; Oganov, A. R. Computational Discovery of Hard and Superhard Materials. *J. Appl. Phys.* **2019**, *126*, No. 040901.
(49) Dubrovinskaia, N.; Dub, S.; Dubrovinsky, L. Superior Wear Resistance of Aggregated Diamond Nanorods. *Nano Lett.* **2006**, *6*, 824−826.
(50) Solozhenko, V. L.; Kurakevych, O. O.; Godec, Y. Le. Creation of Nanostuctures by Extreme Conditions: High-Pressure Synthesis of Ultrahard Nanocrystalline Cubic Boron Nitride. *Adv. Mater.* **2012**, *24*, 1540−1544.
(51) Munro, R. G.; Freiman, S. W.; Baker, T. L. *Fracture Toughness Data for Brittle Materials*; U.S. Department of Commerce, National Institute of Standards and Technology: Gaithersburg, MD, 1998.
(52) Meenaatci, A. T. A.; Rajeswarapalanichamy, R.; Iyakutti, K. Electronic Structure, Structural Stability, Mechanical and Superconducting Properties of Group VB Nitrides: A First Principles Study. *Solid State Sci.* **2013**, *19*, 36−44.

https://doi.org/10.1021/acs.inorgchem.1c00406
Inorg. Chem. XXXX, XXX, XXX−XXX